Structure-dependent band dispersion in epitaxial anthracene films

F. Bussolotti,[a] Y. Yamada-Takamura, Y. Wang, and R. Friedlein[b]
School of Materials Science, Japan Advanced Institute of Science and Technology (JAIST), 1-1, Asahidai, Nomi, Ishikawa 923-1292, Japan

(Received 26 June 2011; accepted 6 September 2011; published online 29 September 2011)

The intermolecular band dispersion related to the highest occupied molecular orbital of epitaxial anthracene multilayer films on single-crystalline Bi(0001) has been measured using angle-resolved ultraviolet photoelectron spectroscopy. By comparing the dispersion to that of anthracene multilayers on Cu(110) [F. Bussolotti, Y. Yamada-Takamura, and R. Friedlein, Phys. Rev. B **80**, 153402 (2009)], it is shown how the transfer integrals and the difference in on-site energies depend on lattice parameters and how this, in turn, affects the band curvature along high-symmetry directions. [doi:10.1063/1.3643717]

INTRODUCTION

Driven by the need to obtain a large charge carrier mobility in organic field-effect transistor devices, there has been recently an increased interest in the understanding of the mechanisms behind the transport of charge carriers in crystalline organic materials, and its relation to electronic and structural properties.[1–6] While transport measurements usually include charge injection or creation processes and the transport through grain boundaries, microscopic parameters related to local and intrinsic properties are best obtained from angle-resolved ultraviolet photoelectron (ARUPS) spectra on well-defined model systems.[7] In this context, of particular interest are the intermolecular band structure, valence binding energy shifts, and the details of the line shape of spectral features related especially to the highest occupied molecular orbital, or HOMO.

Considerable intermolecular band widths W of 400 meV or even higher have been observed for a number of organic thin film and single crystal systems.[5,8–11] In a broad band model ($W > k_BT$, where k_B is the Boltzmann constant and T is the temperature of the system) describing band-like charge transport, the intrinsic hole drift mobility μ_h is inversely proportional to both the effective mass of the hole m_h and W,[7,12] and relates therefore in a straightforward manner to the energy band dispersion at low temperatures. It has been emphasized that the band dispersion depend strongly on the transfer integrals and on the size of the difference of on-site energies ΔE which themselves are determined by details of the crystal structure.[2,3] Experimental results may not always be conclusive and may differ even for films prepared on the same surface. For instance, for pentacene (Pc, see Fig. 1) either monolayers or multilayers with a "standing-up" molecular orientation, three ARUPS studies[5,6,13] show a completely different band dispersion in the *a-b* plane even if as-derived variations of the unit cell are rather small.

In the present paper, by comparing the band dispersions of two epitaxial multilayer films of pentacene's smaller analogue anthracene (Ac, see Fig. 1), prepared on either Bi(0001) or Cu(110),[4] it is shown how the balance of transfer integrals and ΔE depend on lattice parameters and how these two factors, in turn, affect the band dispersion along high-symmetry directions. In particular, it is found that under certain conditions, contributions from nearest-neighbour transfer integrals may largely cancel each other. As a consequence, flattening of the upper HOMO band will cause a reduction of the charge carrier mobility.

EXPERIMENTAL

Single-crystalline Bi(0001) surfaces have been prepared under ultra-high vacuum conditions by deposition of a 10-nm-thick Bi films onto clean Si(111)-7×7 surfaces as described in Refs. 14 and 15. Samples have been annealed at 380 K to improve the morphology of the Bi(0001) films.[14] Single-crystallinity was confirmed by the appearance of the characteristic electron diffraction pattern obtained by reflection high-energy electron diffraction (RHEED),[16] shown in Fig. 1(a). Multilayer Ac films (30 Langmuirs of total exposure) have been deposited *in situ* onto these Bi(0001) surfaces kept at 140 K, using a procedure described previously.[17] ARUPS spectra have been acquired using a Scienta SES-100 analyzer, with an angular and total energy resolution of 0.2° and less than 50 meV, respectively. The samples have been excited by unpolarized HeI photons ($h\nu = 21.218$ eV). For RHEED, the electron energy of 15 keV and an emission current of 28 μA have been employed.

RESULTS AND DISCUSSION

After deposition of the anthracene multilayer, valence band ARUPS features characteristic of the thin film metal substrate (not shown) are completely suppressed which is consistent with an anthracene film thickness of at least 3 nm. A selection of multilayer RHEED patterns is reported in Fig. 1(a). In order to reconstruct the lateral periodicity of the outermost

[a]Present address: Graduate School of Advanced Integration Science, Chiba University, Yahoi-cho, Inage-ku, Chiba 263-8522, Japan.
[b]Author to whom correspondence should be addressed. Electronic mail: friedl@jaist.ac.jp.

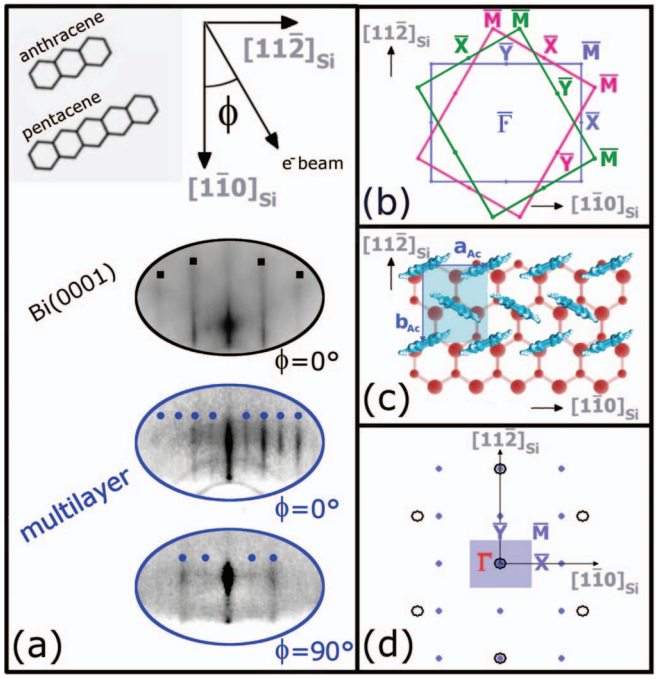

FIG. 1. (a) RHEED pattern images of the Bi(0001) surface (dark filled squares) and of the anthracene multilayer film (blue filled circles) acquired at selected ϕ. In the inset are shown the chemical structures of the anthracene (Ac) and pentacene (Pc) molecules. (b) Reciprocal space representation of the three-domain structure of the Ac multilayer. The surface Brillouin zone (SBZ) of each domain and their relative orientation is explicitly reported. (c) Herringbone-packed molecular arrangement and corresponding unit cell (shaded area) of a single domain with respect to the underlying Bi surface. (d) In-plane reciprocal lattice of a single Ac domain (small filled circles) and of Bi(0001) (large hollow circles). The main crystallographic directions, $\overline{\Gamma X}$, $\overline{\Gamma Y}$, and $\overline{\Gamma M}$, of the organic multilayer SBZ (shaded area) are explicitly indicated.

molecular layer, the electron diffraction images have been acquired in different directions of the incident electron beam identified by the azimuthal angle ϕ with respect to the Si [1$\bar{1}$0] main crystallographic axis'. At $\phi = 0°$ and $\phi = 90°$, within the error bars, the diffraction pattern is similar to that reported for pentacene on Bi(0001) indicating the presence of a thin film of standing molecules which is isostructural in the *a*-*b* plane to the so-called Pc "thin film" phase.[18,19] RHEED patterns obtained at other values of ϕ (not shown) indicate the existence of rotational domains (Fig. 1(b)) as expected for an epitaxial growth on a hexagonal substrate without uniaxial alignment.

For each domain, the lateral periodicity of the herringbone packed anthracene molecules is well described, as illustrated in Fig. 1(c), in terms of a rectangular surface unit cell with lattice parameters of $a = (6.0 \pm 0.3)$ Å, $b = (7.9 \pm 0.3)$ Å, and $\gamma = 90° \pm 2°$ matching the Bi(0001) surface in a "point-on-line" commensurate relationship. The *a* and *b* axis of the molecular lattice are aligned along the [1$\bar{1}$0] direction and [11$\bar{2}$] direction of the underlying Si(111) substrate, respectively. While the parameter *b* maybe slightly larger than that of the "thin film" phase of pentacene,[18] the structure has a different symmetry as compared to the Pc bulk phase which is monoclinic.[3,6] Note that this new anthracene phase has very different lattice parameters as compared to both the bulk-like crystal ($a = 5.99$ Å, $b = 8.40$ Å)[20] and an epitaxial, single-crystalline phase on Cu(110) ($a = b = 7.3 \pm 0.5$ Å) that we reported recently.[4] Both have, however, within the error bars, a rectangular unit cell.

Focussing on the binding energy region around the HOMO, in Fig. 2(a) is shown the dependence of the ARUPS spectra on the polar angle θ, as acquired along the [11$\bar{2}$] and [1$\bar{1}$0] directions of the Si(111) substrate which are coincident with the $\overline{\Gamma Y}$ and $\overline{\Gamma X}$ directions of one of the six rotational domains of the anthracene film. In order to evaluate the line shape, the spectra have been normalized with respect to the maximum intensity of the HOMO-related peak. Strong changes of the line shape with θ are observed. At least two dispersing features, at the low and higher binding energy side are recognized. These features are denoted H_- and H_+ and are indicated by full lines in Fig. 2(b), respectively. The splitting between H_- and H_+ is too large to account for vibrational satellites,[17] and is, therefore, of electronic origin. The dispersion is clearly different along both directions reflecting the periodicity of the reciprocal lattice shown in Fig. 1(d). It may, therefore, be attributed to the intermolecular dispersion of two HOMO-derived bands.

Note that for localized electronic states related to a particular molecular orbital, the photoelectron emission intensity exhibits a strong angular dependence.[21] Even if extended electronic states are formed as a consequence of intermolecular π–π overlap, as it is the case within the *a*-*b* plane of aromatic crystals with herringbone packing, these states may be localized in directions perpendicular to the π orbitals such that a strong angular dependence of the emission intensity might be observed at angles close to normal of the molecular plane.[22,23] For a single molecular orientation and in such a local picture, the intensity ratio between H_- and H_+ is not expected to change with θ since both features are derived from the same molecular orbital. The same holds along $\overline{\Gamma X}$ and $\overline{\Gamma Y}$ for the molecules on the two inequivalent sites of the rectangular herringbone lattice, since both molecules exhibit the same twist angle with respect to these high-symmetry directions. The applicability of a local picture for the explanation of the emission angle dependence of the HOMO line shape can, therefore, be ruled out.

The superimposition of contributions from other rotational domains is expected to lead to some ambiguity in the interpretation of data. However, from the clear periodicity recognizable in both, the spectra as a function of θ and also as a function of the in-plane electron momentum $k_{\parallel}$ shown in Fig. 2(b), it is obvious that the band edges provide a higher spectral weight making the turning points visible such that the main characteristics of the band dispersion might be discussed. $\overline{\Gamma M}$ directions are only a few degrees off the $\overline{\Gamma Y}$ directions preventing an evaluation along this direction.

The band dispersion along $\overline{\Gamma X}$ and $\overline{\Gamma Y}$ bears some characteristic similarities but also differences to that of the Ac phase on Cu(110), at similar temperatures.[5] In both cases, the largest splitting between the H_+ and H_- bands is observed at the $\overline{\Gamma}$ point while it is smaller at the $\overline{X}$ and $\overline{Y}$ points. For Ac on Bi(0001), the H_- band width is very small ($W < 30$ meV) while it is about 60 meV for Ac on Cu(110).[4] For both

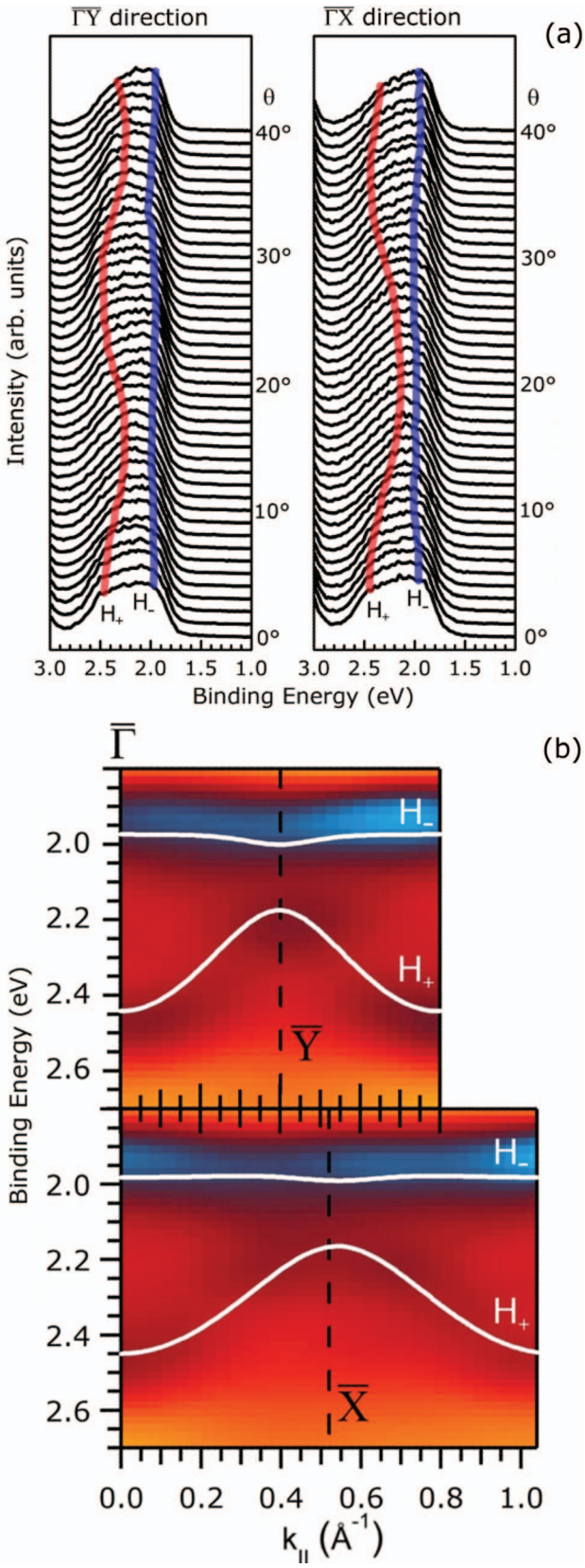

FIG. 2. (a) Dependence of the ARUPS spectra of the anthracene/Bi(0001) multilayer film on θ, along the $\overline{\Gamma X}$ and $\overline{\Gamma Y}$ directions. The binding energy of H_+ and H_- is indicated by thick lines. (b) The second derivatives of the raw spectra plotted in the colour contrast, as a function of $k_\parallel$. Solid white lines represent dispersions as obtained by a TB analysis.

TABLE I. Lattice and 2D tight-binding parameters obtained from a fit to the experimental band structure of the anthracene/Bi(0001) and anthracene/Cu(110) (Ref. 4) films. The negative energy scale is employed to allow comparison with literature data.

	Ac/Bi(0001)	Ac/Cu(110) (spectra in Ref. 4)
a (Å)	6.0 ± 0.3	7.3 ± 0.5
b (Å)	7.9 ± 0.3	7.3 ± 0.5
γ (○)	90 ± 2	90
E_0 (meV)	−2150	−2352
ΔE (meV)	174.1	259.5
t_a (meV)	−34.5	−8.1
t_b (meV)	−30.0	−8.1
$t_{(a+b)/2}$ (meV)	48.4	50.3
$t_{(a-b)/2}$ (meV)	60.2	50.3
t_{2a} (meV)	2.1	1.7
t_{2b} (meV)	1.4	1.7

systems, the H_+ bands have a width significantly larger than those of the H_- bands.

While over here it shall not be claimed that a two-dimensional (2D) tight-binding (TB) model contains the full physics behind the band dispersion, it can provide parameters that will facilitate the comparison of the two phases in its relation to the in-plane crystal structure. In this model, the energy dispersions of the two bands are given by

$$E_\pm(\mathbf{k}) = E_0 + 2\sum_i t_i \cos(\mathbf{k}\cdot\mathbf{r}_i) \pm \left[\left(2\sum_j t_j \cos(\mathbf{k}\cdot\mathbf{r}_j)\right)^2 + (\Delta E/2)^2\right]^{1/2}, \quad (1)$$

where $\mathbf{k}$ is the wave vector, ΔE is the energy difference between the two inequivalent sites, and E_0 is the average of the two on-site energies.[3,5] The transfer integrals t_i and t_j relate to exchanges between molecules in the same or different sublattices, $\mathbf{r}_i$ and $\mathbf{r}_j$ are the vectors defining the intermolecular separations. In Table I are shown the results of a curve fitting of the observed band dispersions of the two Ac phases using the 2D TB approximation with the least squared deviation.

First, for both Ac phases, the transfer integrals between adjacent molecules inequivalent sites, $t_{(a+b)/2}$ and $t_{(a-b)/2}$, are of similar sign as typical for the "thin film" phase of pentacene,[5] but different to the so-called "bulk" phase[6] where the molecules are displaced from each other along the molecular axis.[4] The size of these nearest-neighbour transfer integrals in the two Ac phases is found to be of comparable magnitude. Transfer integrals within the same sub-lattice, t_a and t_b, however, depend strongly on the lattice parameters a and b. In absolute numbers, t_a and t_b are very small for Ac/Cu(110). Both values are about three time smaller than those for Ac/Bi(0001). An equal size of t_a and t_b in Ac/Bi(0001) may not be expected since the lattice constants a and b are very different from each other.

As shown in Fig. 3(a) for the $\overline{\Gamma X}$ direction of Ac/Bi(0001) and the corresponding direction for Ac/Cu(110),[24] these large differences in t_a and t_b determine details of the band width and dispersion of the H_+ band. If the transfer integrals within the same sub-lattice vanish (and if second-nearest neighbour contributions are

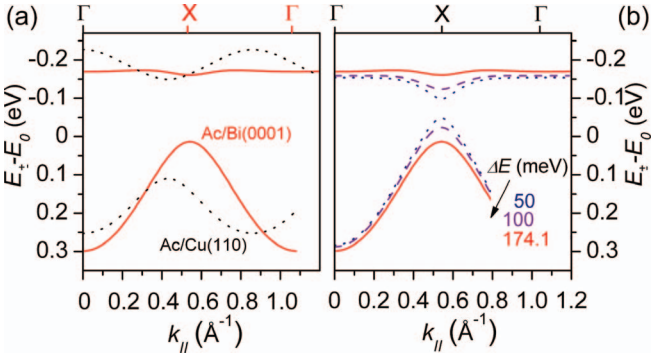

FIG. 3. (a) 2D TB fit to the band dispersion $E_{\pm}$ ($k_{\parallel}$) along the $\overline{\Gamma - X - \Gamma}$ directions of the H_+ and H_ bands of the anthracene/Bi(0001) thin film (full) as compared to the corresponding direction of the anthracene/Cu(110) multilayer film (dotted) (Ref. 21). (b) 2D TB band dispersion for Ac/Bi(0001) (full) and for other values of ΔE of 100 meV (magenta, dashed) and 50 meV (dotted). E_0 has been subtracted from the binding energy.

small), as it is the case for Ac/Cu(110), the H_+ band adapts a cosine-like dispersion with a relatively small band width determined by the transfer integrals to the other sub-lattice, $t_{(a+b)/2}$ and $t_{(a-b)/2}$. For Ac/Bi(0001), on the other hand, contributions from t_a and t_b cancel largely those from $t_{(a+b)/2}$ and $t_{(a-b)/2}$ such that H_+ becomes flat. Contributions from overlap integrals to second-nearest neighbours of the same sub-lattice, t_{2a} and t_{2b}, are negligible. Note that it has been considered that the observed enhancement of t_{2a} and t_{2b} in pentacene monolayer films maybe related to the coupling of the monolayer to the Bi substrate.[5] This would require hybridization between molecular π and substrate orbitals which is not expected and observed in our multilayer films.

Next, differences in on-site energies, ΔE, vary to some extent between the two Ac phases. As discussed by Valeev *et al.*,[25] for "face-to-edge" aligned molecules present in herringbone structures, the origin of the energy splitting ΔE is largely caused by polarization effects than by contributions from transfer integrals that dominate for the parallel molecular orientation. For the size of ΔE, polarization effects of the nearest-neighbour "face-to-edge" interactions cancel to quite some extent, the exact amount depending on the exact topology.[25] In particular, this polarization certainly depends sensitively on the tilt angle between molecules in different sub-lattices, the so-called "herringbone angle," and on the distance between those molecules. Both values will change if the square-like unit cell of Ac/Cu(110) is elongated in one and shortened in the other direction, as it is for Ac/Bi(0001).

Finally, it is discussed how the size of ΔE influences the HOMO band dispersion. In Fig. 3(b), are plotted the H_+ and H_ band dispersions of the anthracene phase on Bi(0001), for various values of ΔE. As understandable from Eq. (1), increasing ΔE flattens the bands slightly. It is clear that changes in ΔE have, however, only a minor impact on the band dispersion and the charge carrier transport if $t_{(a+b)/2}$ and $t_{(a-b)/2}$ are sufficiently large.

CONCLUSIONS

In summary, the comparison of the measured HOMO band structure of two anthracene phases is found to provide information on the evolution of extended electronic states in quasi-2D thin films of herringbone-arranged poly-aromatic systems as a function of the crystal structure. For the films discussed here, a 2D tight-binding description seems to represent well the observed band dispersions. It is revealed that the balance between nearest neighbour transfer integrals plays a decisive role, while differences in the on-site energies are less important in determining the curvature of the HOMO-derived bands. Structure-dependent differences of transfer integrals between the same and different sub-lattices are then also expected to strongly influence the charge transport in organic high-mobility materials.

ACKNOWLEDGMENTS

We acknowledge financial support from Special Coordination Funds for Promoting Science and Technology commissioned by MEXT, Japan, and from "The grant of the MAZDA Foundation," as well as for F.B. for a JSPS Fellowship and Y.W. for a fellowship from the MARUBUN Foundation.

[1] W.-Q Deng and W. A. Goddard III, J. Phys. Chem. B **108**, 8614 (2004).
[2] V. Coropceanu, J. Cornil, D. A. da Silva Filho, Y. Olivier, R. Silbey, and J.-L. Brédas, Chem. Rev. **107**, 926 (2007).
[3] H. Yoshida and N. Sato, Phys. Rev. B **77**, 235205 (2008).
[4] F. Bussolotti, Y. Yamada-Takamura, and R. Friedlein, Phys. Rev. B **80**, 153402 (2009).
[5] M. Ohtomo, T. Suzuki, T. Shimada, and T. Hasegawa, Appl. Phys. Lett. **95**, 123308 (2009).
[6] R. C. Hatch, D. L. Huber, and H. Höchst, Phys. Rev. B **80**, 081411(R) (2009).
[7] N. Ueno and S. Kera, Prog. Surf. Sci. **83**, 490 (2008).
[8] S. Hasegawa, T. Mori, K. Imaeda, S. Tanaka, Y. Yamashita, H. Inokuchi, H. Fujimoto, K. Seki, and N. Ueno, J. Chem. Phys. **100**, 6969 (1994).
[9] X. Crispin, J. Cornil, R. Friedlein, K. K. Okudaira, V. Lemaur, A. Crispin, G. Kestemont, M. Lehmann, M. Fahlman, R. Lazzaroni, Y. Geerts, G. Wendin, N. Ueno, J.-L. Brédas, and W. R. Salaneck, J. Am. Chem. Soc. **126**, 11889 (2004).
[10] R. Friedlein, Y. Wang, A. Fleurence, F. Bussolotti, Y. Ogata, and Y. Yamada-Takamura, J. Am. Chem. Soc. **132**, 12808 (2010).
[11] S. I. Machida, Y. Nakayama, S. Duhm, Q. Xin, A. Funakoshi, N. Ogawa, S. Kera, N. Ueno, and H. Ishii, Phys. Rev. Lett. **104**, 156401 (2010).
[12] H. Fröhlich and G. G. Sewell, Proc. Phys. Soc. London **74**, 643 (1959).
[13] H. Kakuta, T. Hirahara, I. Matsuda, T. Nagao, S. Hasegawa, N. Ueno, and K. Sakamoto, Phys. Rev. Lett. **98**, 247601 (2007).
[14] S. Yaginuma, T. Nagao, J. T. Sadowski, A. Pucci, Y. Fujikawa, and T. Sakurai, Surf. Sci. **547**, L877 (2003).
[15] C. R. Ast and H. Höchst, Phys. Rev. Lett. **87**, 177602 (2001).
[16] A. Al-Mahboob, J. T. Sadowski, T. Nishihara, Y. Fujikawa, Q. K. Xue, K. Nakajima, and T. Sakurai, Surf. Sci. **601**, 1304 (2007).
[17] F. Bussolotti, S. W. Han, Y. Honda, and R. Friedlein, Phys. Rev. B **79**, 245410 (2009).
[18] J. T. Sadowski, G. Sazaki, S. Nishikata, A. Al-Mahboob, Y. Fujikawa, K. Nakajima, R. M. Tromp, and T. Sakurai, Phys. Rev. Lett. **98**, 046104 (2007).
[19] T. Shimada, M. Ohtomo, T. Suzuki, T. Hasegawa, K. Ueno, S. Ikeda, K. Saiki, M. Sasaki, and K. Inaba, Appl. Phys. Lett. **93**, 223303 (2008).
[20] C. P. Brock and J. D. Dunitz, Acta Crystallogr. B **46**, 795 (1990).
[21] S. Kera, S. Tanaka, H. Yamane, D. Yoshimura, K. K. Okudaira, K. Seki, and N. Ueno, Chem. Phys. **325**, 113 (2006).
[22] R. Friedlein, X. Crispin, C. D. Simpson, M. D. Watson, F. Jäckel, W. Osikowicz, S. Marciniak, M. P. de Jong, P. Samorí, S. K. M. Jönsson, M. Fahlman, K. Müllen, J. P. Rabe, and W. R. Salaneck, Phys. Rev. B **68**, 195414 (2003).
[23] S. Berkebile, P. Puschnig, G. Koller, M. Oehzelt, F. P. Netzer, C. Ambrosch-Draxl, and M. G. Ramsey, Phys. Rev. B **77**, 115312 (2008).
[24] Marked as $\overline{\Gamma M}$ in Ref. 4.
[25] E. F. Valeev, V. Coropceanu, D. A. da Silva Filho, S. Salman, J.-L. Brédas, J. Am. Chem. Soc. **128**, 9882 (2006).